CO Oxidation and Site Speciation for Alloyed Pd-Pt Model Catalysts Studied by *in situ* FTIR Spectroscopy

Natalia M. Martin,[*,†] Magnus Skoglundh,[†] Gudmund Smedler,[‡] Agnes Raj,[¶] David Thompsett,[¶] Peter Velin,[†] Francisco J. Martinez-Casado,[§] Zdenek Matej,[§] Olivier Balmes,[§] and Per-Anders Carlsson[†]

†*Competence Centre for Catalysis, Chalmers University of Technology, Gothenburgh, 412 96, Sweden*

‡*Johnson Matthey AB, Västra Frölunda, 421 31, Sweden*

¶*Johnson Matthey Technology Centre, Blounts Court, Sonning Common, Reading, RG4 9NH, UK*

§*MAX-IV Laboratory, Lund University, Lund, 221 00, Sweden*

E-mail: Natalia.Martin@chalmers.se

Phone: +46 (0)31-772 29 04.

Abstract

In situ Fourier transform infrared spectroscopy was used to study transient CO oxidation over a series of bimetallic Pd-Pt catalysts with different Pd:Pt molar ratios. The catalysts were found to contain both alloyed PdPt nanoparticles (particle sizes 25-35 nm) and monometallic Pd nanoparticles (sizes below 10 nm). For oxygen-free conditions, CO reduces the surface while simultaneously function as a chemical probe molecule whereby the CO adsorption sites can be characterised. Under these conditions it is shown that adsorbed carbonyl species form both on the Pd and Pt. On platinum, CO adsorbs predominantly linearly on top, whereas on palladium it adsorbes in bridged configurations. This behaviour is used for site speciation of the catalysts. The spectra from the bimetallic Pd-Pt catalysts are more complicated than a direct superposition of the spectra for the monometallic catalysts as a consequence of alloy formation and enrichment of Pd at the surface of the reduced catalysts. The temperature programmed CO oxidation results show that the addition of Pd to the Pt catalyst supported on alumina shifts the CO-poisoned state to lower temperatures therefore increasing the temperature range for the CO oxidation at low temperatures.

Introduction

Oxidation of carbon monoxide is one of the most studied catalytic reactions in heterogeneous catalysis not only for its importance in environmental applications such as automotive emission control but also for its use as probe reaction in the development of new catalysts. Further, CO is a suitable molecule for characterisation of surfaces and probing of different binding sites on catalytic surfaces.[1,2] Both the CO/Pd and CO/Pt systems have previously been studied by several groups, as summarised in references[1–8] and references therein. The results indicate that CO adsorbs mainly linearly on atop surface sites on Pt surfaces while for Pd surfaces hollow sites are preferred at low CO coverages and bridge/on-top sites are populated at higher coverages.[1] For bimetallic Pd-Pt catalysts, however, less work has been devoted to CO adsorption and the characterisation of their surface structure using CO as probe molecule.

We study bimetallic palladium-based catalysts used in various reactions such as oxidation of hydrocarbons,[9–18] hydrodesulfurization,[19] or hydrodeoxygenation,[20] because of their enhanced activity compared to monometallic Pd or Pt catalysts. The properties of bimetallic catalysts are often different from those of the constituent components with high structural complexity. Often a preferential distribution of Pd atoms at the nanoalloys surface has been observed both experimentally[21] and theoretically[22,23] for the Pd-Pt nanoparticles. A review of the effect of metal addition to Pd-based catalysts has previously been presented by Coq and Figueras.[24]

Recent studies have demonstrated that the structure, composition, and chemical state of the surface of bimetallic catalysts play a critical role in determining their catalytic properties. The surface composition of alloys, in particular the composition of the topmost surface layer, is generally different from the bulk composition due to segregation processes.[25–27] Several studies on Pt-Pd bimetallics dispersed on a support have reported segregation of Pd on the surface of bimetallic particles under both oxidative or reducing environments even thought the alloy formation has not always been questioned.[28–31]

Previously, we have studied the influence of temperature and atmosphere during catalyst calcination on the alloy formation and oxidation/reduction behaviour of bimetallic Pd-Pt catalysts supported on alumina containing 2 wt.% Pd and 0.4 wt.% Pt using a combination of X-ray absorption spectroscopy (XAS), low-energy ion scattering spectroscopy (LEIS), transmission electron microscopy (TEM) and X-ray diffraction (XRD).[32] It was shown that bimetallic Pd-Pt nanoparticles alloy is evident in the catalysts calcined at 800 °C, both in dry and wet air. In addition to alloy nanoparticles, these samples show the presence of smaller Pd nanoparticles. Further, the bimetallic nanoparticles were found to expose a Pd-Pt metallic surface under reducing conditions (Pd enriched), while under oxidising conditions, a PdO phase dominates the surface. No alloy formation was observed for the catalyst calcined at 500 °C, but individual monometallic Pd or Pt nanoparticles that are oxidised to PdO and PtO_x under oxidising conditions.

Further, the same series of bimetallic Pd-Pt catalysts showed a similar behaviour of the alloyed nanoparticles during lean and rich methane oxidation conditions as previously observed during oxidation and reduction treatments.[9] *In situ* diffusive reflectance infrared Fourier transform spectroscopy (DRIFTS) measurements showed the formation of adsorbed carbonyl species during rich conditions over the catalysts and the measurements indicate that the non-alloyed nanoparticle sample (calcined at 500 °C) exposes both Pd and Pt during reaction conditions, while the samples calcined at 800 °C mainly expose Pd, which is easily oxidised to PdO under lean conditions. The measurements suggested that using CO as probe molecule combined with an easy-available characterisation method such as DRIFTS may provide a clear evidence of alloy formation in bimetallic catalysts.

In the present work, transient CO oxidation has been studied over a series of bimetallic Pd-Pt catalysts and their surface structure has been characterised by *in situ* DRIFT spectroscopy using CO as probe molecule. Particular focus is paid on the formation on carbonyl species during oxygen-free conditions. The catalysts contain alloyed nanoparticles with different metal loadings and Pd:Pt molar ratios and were initially calcined in air at 800

°C, since our previous results indicated the existence of PdPt alloy at 800 °C for a similar system.[32]

Experimental section

Catalyst preparation and *ex situ* characterisation

Model catalysts (from here referred to as catalysts) with different Pd and Pt loadings supported on γ -Al_2O_3 were prepared by incipient wetness impregnation followed by calcination in air 800 °C for 10 h. For comparison, additional samples containing either 2.0 or 0.4 wt.% Pd or Pt were prepared. The different samples are summarised in Table 5. For simplicity, the samples will hereafter be referred to by their sample ID.

Inductively coupled plasma optical emission spectroscopy (ICP-OES) analysis was used to confirm the noble metal content of all samples.

Table 1: Nomenclature for the catalyst samples used in this study.

Sample ID	Molar ratio Pd:Pt	Metal content		ICP metal content		Assay metal content	Alloy composition
		Pd (wt.%)	Pt (wt.%)	Pd (wt.%)	Pt (wt.%)	Pd:Pt (at.%)	Pd:Pt (at.%)
2 Pd-0.4 Pt	9:1	2.0	0.4	1.76	0.35	89:11	54:46
1.2 Pd-1.2 Pt	2:1	1.2	1.2	1.10	1.10	63:37	51:49
0.4 Pd-2 Pt	0.4:1	0.4	2.0	0.36	1.81	25:75	15:85
2 Pt	-	-	2.0	-	1.77	-	-
0.4 Pt	-	-	0.4	-	0.36	-	-
2 Pd	-	2.0	-	1.77	-	-	-
0.4 Pd	-	0.4	-	0.37	-	-	-

The crystal structure and alloy formation of the samples were studied by X-ray diffraction at beamline I711 at the MAX IV Laboratory in Lund, Sweden,[33,34] using a Newport diffractometer equipped with a Pilatus 100K area detector, at a fixed wavelength (λ = 0.9941 Å). The detector was scanned continuously from 0 to 120° in approximately 20 min, recording 125 images/° (step size of 0.008°). The true 2-theta position of each pixel was recalculated, yielding an average number of 100000 pixels contributing to each 2-theta value. The samples, contained in 0.3 mm spinning capillaries, were measured in transmission mode.

In situ Fourier transform infrared spectroscopy

The *in situ* Fourier transform infrared spectroscopy measurements were performed in diffuse reflectance mode with a BRUKER Vertex 70 spectrometer equipped with a high-temperature stainless steel reaction cell (Harrick Praying Mantis^{TM} High Temperature Reaction Chamber) with KBr windows and a nitrogen-cooled MCT detector. The reaction cell contains a sample cup with a diameter of 6 mm and a depth of 3 mm. The wavenumber region between 1700-2500 cm^{-1} was measured with a spectral resolution of 2 cm^{-1} and a time resolution of about 1.5 s. The temperature of the sample holder was measured by a thermocouple (type k) and controlled by a PID regulator (Eurotherm). Feed gases were introduced into the reaction cell via individual mass flow controllers, providing a total flow of 100 ml/min in all experiments. Prior to the temperature ramp experiments, each sample was pre-treated at 250 °C in a flow of H_2 for 10 min and subsequently in a flow of O_2 for 10 min. An IR background was recorded after the sample was reduced in H_2. The sample was then exposed to 0.1%CO+2%O_2 and the temperature was decreased in steps of 5 °C/min to 50 °C and finally increased to 250 °C after 10 min at 50 °C.

For the CO oxidation step response experiments the sample was pre-treated with a net-oxidising CO/O_2/Ar feed for 20 min at the actual temperature to be studied and then a background spectrum was collected of the sample in the feed since it will contain no absorption bands for CO bonded to the nobel metal particles under oxidising conditions. Two different measurement series of transient CO oxidation over the different Pt, Pd and Pd-Pt catalysts at different CO/O_2 ratios were performed as described in Table 2. In the first series, the samples were exposed to 0.1%CO/1%O_2/Ar for 60 s, followed by a exposure to 0.1%CO/Ar flow for 300 s (reduction phase) and then exposure to 0.1%CO/1%O_2/Ar for another 240 s (oxidation phase) at three different temperatures (350, 250 and 150 °C). In the second experimental series, the CO concentration was increased to 1% and the experiment was repeated at 250 °C under otherwise the same reaction conditions. The product stream was continuously analysed by mass spectrometry (Hidden Analytical, HPS-20 QIC) following

the m/e ratios 2 (H_2), 15 and 16 (CH_4), 18 (H_2O), 28 (CO), 40 (Ar) and 44 (CO_2).

Table 2: Summary of step response experimental conditions for the DRIFTS experiments.

Experiment	Gas composition	Duration	Process
E1	0.1%CO/1%O2/Ar	20 min	Pre-treatmnent
	0.1%CO/1%O2/Ar	60 s	
	0.1%CO/Ar	300 s	Reduction phase
	0.1%CO/1%O2/Ar	240 s	Oxidation phase
E2	1%CO/1%O2/Ar	20 min	Pre-treatmnent
	1%CO/1%O2/Ar	60 s	
	1%CO/Ar	300 s	Reduction phase
	1%CO/1%O2/Ar	240 s	Oxidation phase

Results and discussion

Ex situ characterisation of as-prepared samples

The metal loadings of Pd and Pt of the catalysts have been determined from the ICP-OES (shortly ICP) and are presented in Table 1. It can be observed that the actual metal loadings are very similar to the theoretically expected values.

X-ray diffraction patterns were recorded for each of the samples to investigate both the presence and crystallinity of different phases as well as the apparent crystal size of catalyst particles. Fig. 1 shows the XRD patterns for the as-prepared Pd, Pt and Pd-Pt/Al_2O_3 catalysts calcined at 800 °C in air. The Pd/Al_2O_3 catalysts show the presence of Al_2O_3 (denoted by black and green lines at the bottom) and PdO (denoted by red lines), while the Pt/Al_2O_3 catalysts show the presence of metallic Pt (denoted by blue lines) in addition to alumina. The different reflections were assigned using the ICSD data for Pd, Pt, PdO and alumina at a wavelength of 0.9941 Å.[35] The PdO peaks are relatively broad implying that PdO are highly dispersed over the surface of the support. A clear analysis of the XRD data suggests the support to be a mixture of different alumina phases for all samples, even though the gamma phase dominates the diffraction patterns.

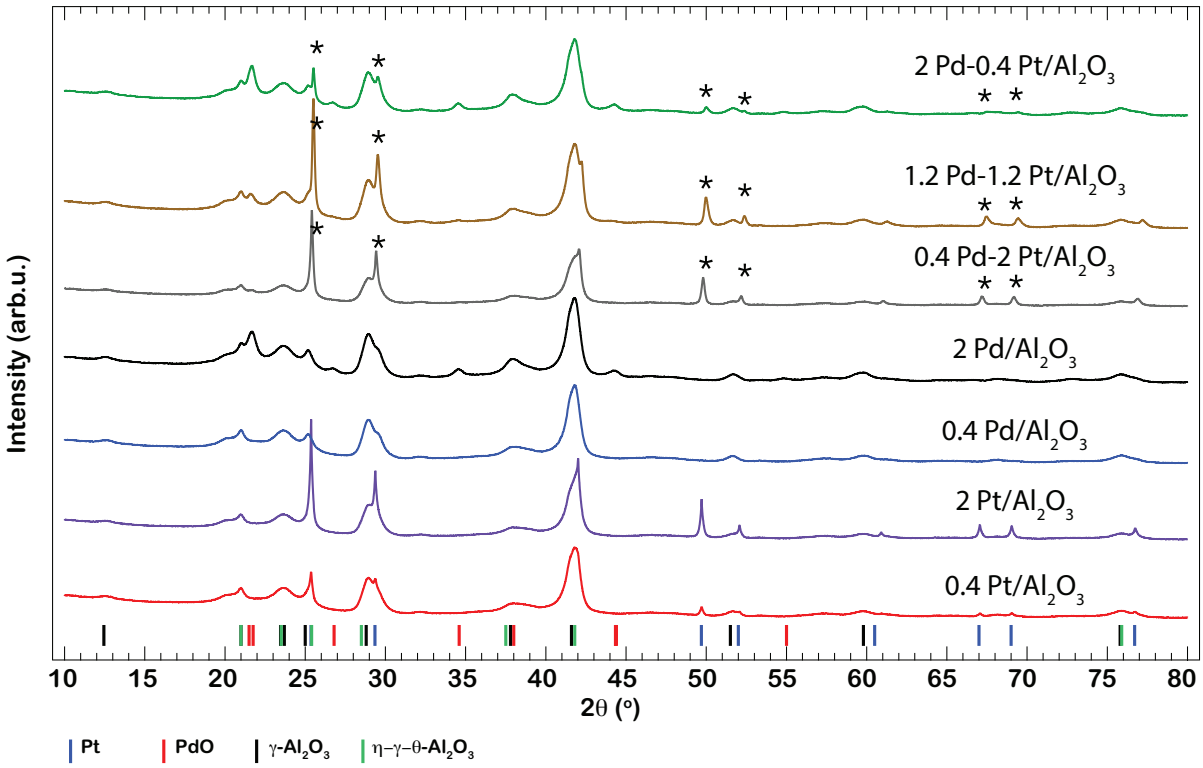

Figure 1: XRD patterns of as-prepared Pd, Pt and Pd-Pt catalysts supported on Al_2O_3 and calcined at 800 °C in air. The coloured bars at the bottom represent the reflections calculated using the ICSD database for Pt (blue), PdO (red), and alumina (black- γ phase and green- combination of η-γ-θ phases).

For the bimetallic Pd-Pt samples no peaks due to metallic Pt or Pd are observed in addition to alumina, but PdO reflections and additional reflections (denoted by *) which are attributed to Pd-Pt scattering, similar to the results presented in our previous publication.[32] We find the strongest new reflections to appear at 25.25 and 29.25° for the 2 Pd-0.4 Pt and 1.2 Pd-1.2 Pt samples, while they are slightly shifted towards metallic Pt for the 0.4 Pd-2 Pt sample (25.15° and 29.15°), suggesting that the structure of the alloy Pt-Pd nanoparticles in this sample is similar to the Pt nanoparticle sample. The new reflections are sharp for the 1.2 Pd-1.2 Pt and 0.4 Pd-2 Pt samples suggesting larger crystallites as compared to the 2 Pd-0.4 Pt sample where broader Pd-Pt reflections are observed. Further, only minor amounts of PdO are observed for the bimetallic samples with Pd:Pt molar ratio equal or lower than 2:1, suggesting that palladium is well dispersed in these samples.

The full width at half maximum (FWHM) values of the characteristic peaks of PdO(101) (2θ= 21.7°), Pt(111) (2θ= 25°) and Pd-Pt (2θ= 25.25° or 25.15°) are used to calculate the apparent crystallite sizes, using Scherrer's equation[36] (t = K*λ / (B(2θ)*cos(θ)), where t= apparent size of the ordered domains, λ=0.9941 Å, B(2θ)=FWHM, θ=Bragg angle, K=0.89, the shape factor), and the results are listed in Table 3. An increase in the PdO crystallite size is observed for the Pd-Pt catalysts compared to the Pd catalyst containing the same amount of Pd, while, for the Pd-Pt catalysts, less sintering of Pd-Pt crystallites is observed compared to Pt crystallites of the Pt monometallic catalysts. Lowering the amount of Pd or Pt in the bimetallic samples will result in smaller crystallites.

CO oxidation over bimetallic Pd-Pt/alumina model catalysts

Temperature programmed CO oxidation

The CO oxidation was performed under a flow of 0.1%CO+2%O_2 while the temperature was reduced from 250 °C to 50 °C in steps of 5 °C/min and then increased to 250 °C after 10 min at 50 °C. Figure 2 shows the time evolution of the IR bands in the interval 1700-2500 cm^{-1} during the cooling and heating in a flow of CO+O_2 for the bimetallic samples

Table 3: Apparent particle sizes calculated from XRD patterns using Scherrers equation at a wavelength $\lambda = 0.9941$ Å.

Sample ID	Pd:Pt (wt.%)	2θ PdO (°)	d_{PdO} (nm)	2θ Pd-Pt (°)	d_{Pd-Pt} (nm)	2θPt (°)	d_{Pt} (nm)
2 Pd-0.4 Pt	2:0.4	21.7	11.0	25.25	26.0	-	-
1.2 Pd-1.2 Pt	1.2:1.2	21.7	5.0	25.25	30.0	-	-
0.4 Pd-2 Pt	0.4:2	21.7	<5.0	25.15	31.0	-	-
2 Pt	0:2	-	-	-	-	25.0.0	33.0
0.4 Pt	0:0.4	-	-	-	-	25.0	27.0
2 Pd	2:0	21.7	7.5	-	-	-	-
0.4 Pd	0.4:0	-	-	-	-	-	-

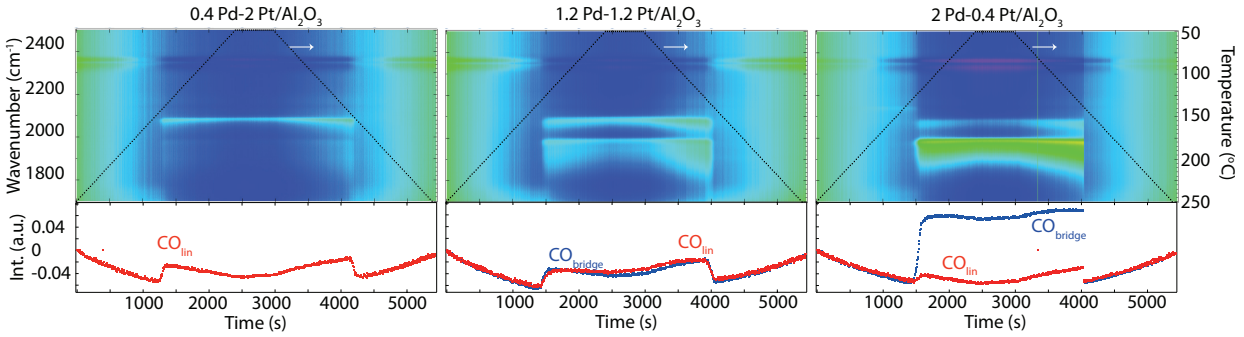

Figure 2: Time resolved IR absorption spectra in the wavenumber region 1700-2500 cm^{-1} for the Pd-Pt catalysts supported on Al_2O_3 and calcined at 800 °C in air and exposed to 0.1%CO+2%O_2 while the temperature has been reduced from 250 °C to 50 °C in steps of 5 °C/min and then increased back to 250 °C after staying at 50 °C for 10 min for the 0.4 Pd-2Pt (left panels), 1.2 Pd-1.2 Pt (middle panels) and 2 Pd-0.4 Pt (right panels) catalysts. Bottom: Intensity of the CO adsorption band at 2083 cm^{-1} (linear) or 1983 cm^{-1} (bridge).

together with the integrated peak intensity for the adsorbed CO species (linear and bridge configurations) formed during the measurement. Formation of CO_2 in the gas phase can be detected in the IR spectra at temperatures above ∼160 °C (bands centred at 2350 cm^{-1}) for all samples indicating the proceeding reaction. The CO_2 bands disappear for temperatures below ∼160 °C when CO adsorption is observed. This is confirmed by the mass spectrometry data presented in Figure S1 in the Supplementary Information. Table 4 shows the formation temperature of CO adsorbed species for the different bimetallic catalysts during the temperature programmed CO oxidation measurements both during cooling and heating ramps. The differences observed between the different samples may be explained by a size-dependent effect of Pd nanoparticles: smaller particles will be completely oxidized (0.4 Pd-2 Pt sample), whereas for the samples with intermediate particles sizes partial oxidation takes place (1.2Pd-1.2Pt and 2Pd-0.4Pt samples) and can, therefore, be reduced faster.[37]

Carbon monoxide and oxygen adsorb competitively, where CO adsorption is favored at low temperatures as seen in the FTIR spectra by the formation of CO adsorbed species. This gives rise to the hysteresis behavior observed for all samples during the heating and cooling ramps, due to the different adsorbates formed during the oxidation (above 160 °C) and reduction (below 160 °C) periods for CO oxidation. For the 0.4 Pd-2 Pt sample, adsorbed CO blocks O_2 dissociation below 150 °C with the appearance of a dominant signal at about 2080 cm^{-1} which has previously been assigned to linearly adsorbed CO on metallic Pt, suggesting that mainly Pt is exposed at the surface of the catalyst reduced by CO. By increasing the Pd content and lowering the Pt metal content, the intensity of the adsorption band for CO on Pd (mainly bridge-bonded CO) increases correspondingly. The assignment of the different bands will be discussed in more detail under the CO adsorption measurements section (3.2.3). The 1.2 Pd-1.2 Pt and 2 Pd-0.4 Pt samples show an increased intensity for the absorption band for bridge-bonded CO on Pd indicating the presence of metallic Pd on the surface during CO oxidation below 130 °C.

Those results indicate that the surface of the bimetallic catalysts is covered by CO below

∼160 °C, with CO adsorbing on both Pd and Pt metallic surfaces. A slight shift of the CO adsorption bands towards lower wavenumbers is observed for all samples during the temperature increase, which is likely due to the decreased CO coverage, *i.e.*, CO-CO lateral interaction.

Table 4: The formation temperature of CO adsorbed species for the different bimetallic catalysts during the temperature programmed CO oxidation measurements.

Catalyst	T ramp down	T ramp up
0.4 Pd-2 Pt	145 °C	155 °C
1.2 Pd-1.2 Pt	130 °C	145 °C
2 Pd-0.4 Pt	125 °C	140 °C

During the low reaction rate regime, the metallic surface is CO covered (the reaction is CO self-poisoned), while in the state with a high reaction rate, no adsorbed CO is observed and the surface of the catalysts is expected to be covered with O species. Only CO adsorption on reduced metal sites is detected during the CO oxidation at low temperatures. This is in agreement with previous studies of CO oxidation over Pt, reporting CO adsorption which poisons Pt sites with respect to oxygen adsorption and therefore inhibits CO oxidation at low temperatures.[38] The results show that the addition of Pd to the Pt catalyst supported on alumina shifts the CO-poisoned state to lower temperatures therefore increasing the temperature range for the CO oxidation at low temperatures. Further, the transition from an O to a CO covered surface occurs slower than the reverse transition from a CO to an O covered surface as also illustrated in Figures S2-S4 in the Supporting Information and as previously reported for Pt.[39] This may indicate that possibly a restructuring of the nanoparticles takes place during CO adsorption as discussed below. The results show that CO can be used as a probe molecule to characterise the surface structure of the nanoparticles at temperatures below ∼150 °C when it accumulates on the surface.

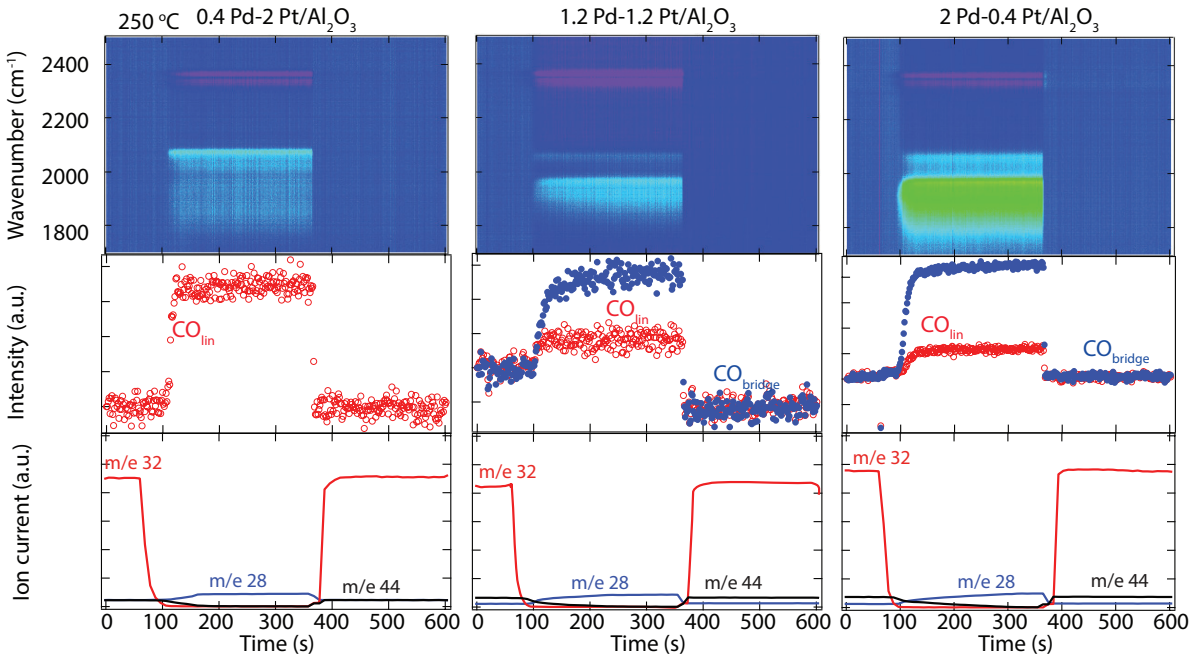

Figure 3: Top: Time resolved IR absorption spectra in the wavenumber region 1700-2500 cm^{-1} for the Pd-Pt catalysts supported on Al_2O_3 and calcined at 800 °C in air and exposed to 0.1% CO + 1% O_2 for 1 min followed by a flow of 0.1% CO for 5 minutes (reduction phase) and 0.1% CO+ 1% O_2 for 4 min (E1) at 250 °C for the 0.4 Pd-2 Pt (left panel), 1.2 Pd-1.2 Pt (middle panel) and 2 Pd-0.4 Pt (right panel) catalysts. The middle panels show the peak intensities for the linearly (red) or bridge-bonded (blue) CO adsorbed on the noble metal nanoparticles, while the bottom panels show the mass spectrometry signals for O_2 (32), CO (28) and CO_2 (44) during the experiment.

Oxygen step-response experiments

Additional experiments were performed to investigate the changes in the oxidation state for the noble metal particles of the bimetallic catalysts during the CO oxidation reaction. The IR results from the first series of the step response experiments (E1 according to Table 2) with 0.1% CO and 1% O_2 at 250 °C are presented in Figure 3 for the bimetallic catalysts with different Pd:Pt molar ratios. Figure 3 shows the time evolution of the absorption bands in the interval 1700-2200 cm^{-1} at 250 °C during step changes of the O_2 concentration for the bimetallic samples together with the integrated peak areas for the carbonyl species formed during the reduction phase. The results of the same series of experiments (E1) performed at 150 and 350 °C are similar to the ones performed at 250 °C and are presented in Figures S2 and S3 (Supporting Information)[†]. A trend from these figures is the formation of clear CO adsorption on metal bands after the O_2 supply has been turned off at t = 60 s. No bands are observed during the oxidation phase and no clear shift is observed in the absorption bands during the reduction phase for any of the samples at each constant temperature. Therefore, we focus the remaining discussion on the results obtained at the end of the reduction phase.

CO adsorption on reduced bimetallic Pd-Pt/alumina model catalysts

Since the transient CO oxidation measurements presented above do not give any information on the oxidation state of the supported particles, *i.e.*, no band of CO adsorbed on the oxidised metal is observed immediately after the switch to oxygen-free conditions, CO is used mainly as probe molecule while it simultaneously acts as a reducing agent.

Selected spectra collected from all investigated samples at the end of the reduction phase (*i.e.*, after the samples have been exposed to 0.1% CO for 5 minutes) are presented in Figure 4 for each constant temperature measurements (150, 250, and 350 °C). During the reduction phase the main absorption bands evolve, corresponding to carbonyl species adsorbed on the nobel metal nanoparticles.

We will start by discussing the results obtained at 150 °C. For the 2 Pt sample, a strong

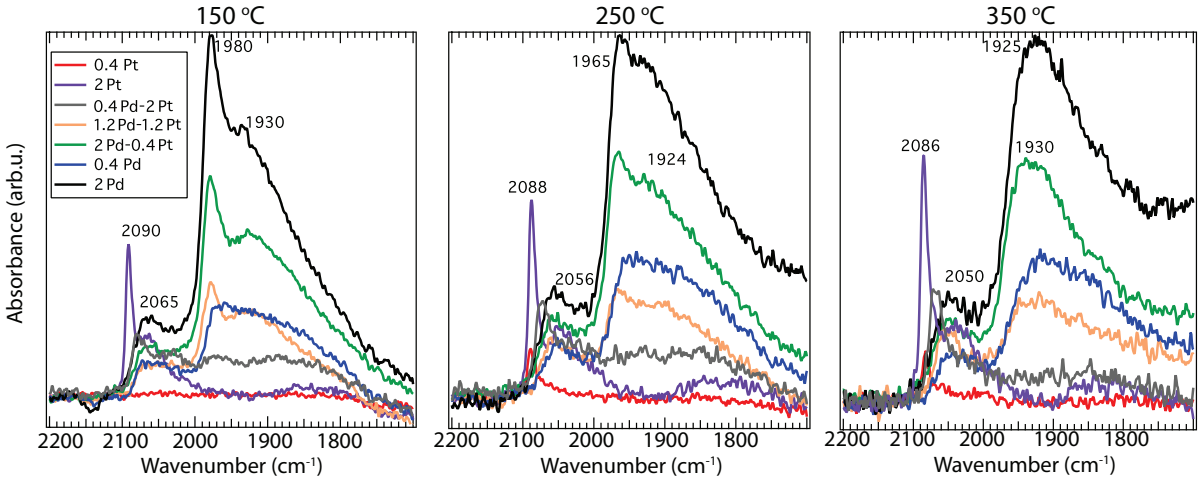

Figure 4: IR absorption spectra in the wavenumber region 1700-2200 cm^{-1} for the Pd, Pt and Pd-Pt catalysts supported on Al_2O_3 and calcined at 800 °C in air and exposed to 0.1% CO for 5 minutes (reduction phase) at 150 °C (left panel), 250 °C(middle panel) and 350 °C (right panel).

Table 5: Assignment of IR absorption bands within the wavenumber region 1800-2200 cm^{-1} observed in this study.

Wavenumber (cm^{-1})	Species	Reference
2070-2090	CO linearly bonded on Pt	[8,39]
1825-1850	Bridge-bonded CO on Pt	[8,39]
2050-2070	CO linearly bonded on Pd	[40,42]
1900-2000	Bridge-bonded CO on Pd	[1,2,40,42]
1850-1900	Three-fold hollow CO on Pd	[1,42]

absorption band around 2090 cm^{-1} with a shoulder on the lower wavenumber side of the maximum is observed together with a weaker broad band around 1825 cm^{-1} after the sample has been exposed to 0.1% CO for 5 minutes (reduction phase) at 150 °C. Those are attributed to linearly adsorbed CO and bridge-bonded CO, respectively, on metallic platinum, as previously assigned[8,39] (Table 5). The shoulder on the lower wavenumber side close to the band from linearly bonded CO is probably due to geometric effects as previously reported for CO adsorption on Pd[40,41] (a high CO coverage reduces the back-bonding capability and leads to a blue-shift of the absorption band).

For the 2 Pd sample, it is interesting to note that there is a strong bonding of CO to bridge sites at particles edges, as observed by the high intensity peak at about 1980-1930 cm^{-1} and previously reported for supported Pd nanoparticles.[1,2,40,42] In addition, a weaker band around 2065 cm^{-1} is observed which has previously been assigned to linearly-bonded CO in metallic Pd[40,42,43] (Table 5). The integrated intensity of the band for bridge-bonded species is significantly higher than that of linear complexes, in agreement with previous reports: CO adsorbs predominantly bridge-bonded on the Pd surfaces, at temperatures above room temperature, therefore the higher intensity of the bridge-bonded component.[42]

For the 0.4% monometallic samples, the intensity of the bands is much weaker compared to the 2% monometallic samples as expected due to the lower content of metal, *i.e.*, lower surface concentration and, therefore, less CO will adsorb.

The spectra of CO adsorbed on the bimetallic catalysts are different than simple superpositions of the spectra of CO adsorbed on the corresponding monometallic Pd and Pt catalysts with different metal contents. As supported by the XRD results, the bimetallic nanoparticle samples contain both alloyed PdPt and smaller Pd nanoparticles (see Table 3). The intensity of the absorption bands for the bimetallic catalysts is lower compared to the monometallic catalysts with similar metal loadings indicating the existence of an interaction between Pd and Pt in the bimetallic samples, which partly affects the CO adsorption as suggested earlier.[12] Another explanation may be the larger particle sizes for the bimetallic

samples compared to the monometallic ones, which will lead to lower metal surface area and therefore less CO adsorption. According to Table 3, the particle sizes are comparable for the monometallic and bimetallic samples, with even less sintering for the bimetallic catalysts, therefore the existence of an interaction between Pd and Pt is a more plausible explanation for this difference. This evidence of alloy formation between Pd and Pt from DRIFTS combined with the XRD results presented above supports our assumptions that the samples calcined at 800 °C contain alloyed nanoparticles. Decreasing the Pt content in the bimetallic samples and increasing the Pd content, induces a decrease of the intensity of the band mainly characteristic of CO adsorbed on Pt (band between 2080-2090 cm^{-1}) while the absorption characteristic of CO adsorbed on Pd (bands below 2000 cm^{-1}) develops progressively. Further, the bimetallic samples containing similar or higher amount of Pt compared to Pd show a broadening of the bands below 2000 cm^{-1}. It is noteworthily mentioning that these changes are even observed on the bimetallic catalysts containing low metal loadings such as 0.4 wt.% metal.

The spectra from the 2 Pd-0.4 Pt and 1.2 Pd-1.2 Pt samples (*i.e.*, Pd:Pt molar ratio of 2:1 or higher), resemble the 2 Pd sample spectra, with a prominent broad band visible below 2000 cm^{-1}, which corresponds to bridge-bonded CO on metallic Pd. Due to a broad signal below 2000 cm^{-1}, it is difficult to observe a possibly small shift in the absorption band positions assigned to CO adsorbed on Pd and even some abundance of threefold coordinated CO on Pd cannot be excluded. The integrated intensity of the band of CO adsorbed on these bimetallic catalysts is much lower than that of the corresponding intensity for the monometallic Pd catalyst and, in addition, no clear band of linearly adsorbed CO on Pt is visible. This can be either due to a particle size effect or an enrichment of Pd at the surface of Pd-Pt alloyed particles. Since the XRD results indicate somewhat larger PdO crystallites for the 2 Pd-0.4 Pt sample and relatively large Pd-Pt particles (26-30 nm) for both samples, this explains partly the decreased intensity of the spectrum of CO adsorbed on the bimetallic catalysts. However, this does not explain the lack of absorption bands corresponding to CO

adsorbed on Pt. Thus, these observations suggest an increased amount of Pd at the surface of the reduced Pd-Pt nanoparticles. This conclusion agrees well with our previous study of oxidation/reduction behaviour on bimetallic Pd-Pt catalysts.[32]

The absorption spectrum for CO adsorbed on the 0.4 Pd-2 Pt sample is quite similar to that of CO absorbed on the monometallic 2 Pt catalyst. It contains two absorption bands with maxima at 2080 cm^{-1} and 2035 cm^{-1}, which are slightly lower wavenumbers than the ones observed for CO adsorbed on pure Pt. This in an interesting observation and indicates some electronic modification of Pt due to alloy formation (ligand effect) as previously reported for a similar system.[41] The alloy formation between Pd and Pt will result in electron density transfer from Pd to Pt, since the electron affinity of Pt is higher than for Pd. Due to the similarity to the corresponding spectrum of CO linearly adsorbed on Pt, the bands at 2080 cm^{-1} and 2035 cm^{-1} most probably correspond to linearly adsorbed CO on surface Pt atoms. Even more, the shift in the CO adsorption band can be due to a restructure of the particles surface during the CO adsorption. Due to a broad signal below 2000 cm^{-1}, even some bridge- or three-fold bonded CO on Pd cannot be excluded, even though it is not possible to determine the maxima in this range. The low intensity is most likely related to a lower dispersion of Pd in the reduced catalyst, also suggested by the XRD results. The surface concentration of Pt in this sample is much lower than in the monometallic 2 Pt catalyst. This cannot be explained by lower particle size, since, according to Table 3, smaller particles are observed for the bimetallic sample. Therefore, one has to conclude that the surface of the alloy particles is enriched with Pd.

Similar results are obtained after repeating the measurements at 250 and 350 °C. A slight shift towards lower wavenumbers is observed for the carbonyl bands as the temperature is increased which is coherent with previous results and discussed elsewhere.[39,41,44,45] In addition, the band for the bridge-bonded CO increases in intensity and sharpens by decreasing the temperature suggesting an increasing coverage on Pd at lower temperatures, while the opposite yields for CO on Pt (increased coverage at higher temperature).

The mass spectrometry data recorded during the FTIR measurements for the E1 experiments are presented in Figure 3 (250 °C) and Figures S2-S3 (150 and 350 °C) (Supporting Information). The data show a similar behavior for all bimetallic catalysts investigated in this study: during the reduction phase, after the O_2 switch (t= 60 s), there is a slow extinction of the CO oxidation reaction for about 100 s as illustrated by the decrease of the m/e 44 and an increase of the m/e 28 signals. During this period a continuous increase of the linearly and bridge bonded CO on metal is seen. The start of this increase depends on the temperature: the lower the temperature the fastest the increase (*i.e.*, at 70 s for 150 °C, 100 s for 250 °C, and 105 s for 350 °C). Both bands increase rather quickly for the first 30 s and then reach a plateau for the remaining time of the reduction phase. At t=360 s the O_2 supply is turned on again (oxidation phase) and the onset of the CO oxidation is indicated by the decrease of the m/e 28 signal and the increase of the m/e 44 signal. The formed carbonyl species decrease and disappear immediately after the O_2 switch. The delay in the formation of carbonyl bands as the temperature is increased may indicate a higher oxidation state of the metal particles which require additional time to be reduced at higher temperatures. By increasing the CO concentration this time shall significantly be reduced as discussed below.

In the second series of IR experiments, the CO concentration was increased by a factor of 10 and the results from the reduction phase at 250 °C are presented in Figure 5. The absorption band for gas phase CO is visible on all spectra between 2100-2200 cm^{-1}. Similar results are obtained as compared to the measurements presented in Figure 4, with a slight shift in frequency of the C-O stretching mode between the two experiments depending on coverage. The complete second series of measurements (E2) for the bimetallic samples at 250 °C are presented in Figure S4 (Supporting Information). Similar to the E1 measurements, no shift of the CO adsorption bands is observed at this temperature. Further, the formation of carbonyl species takes place earlier (70 s) after the O_2 has been switched off compared to the same experiment at lower CO concentration (100 s) as described above for the E1

experiment.

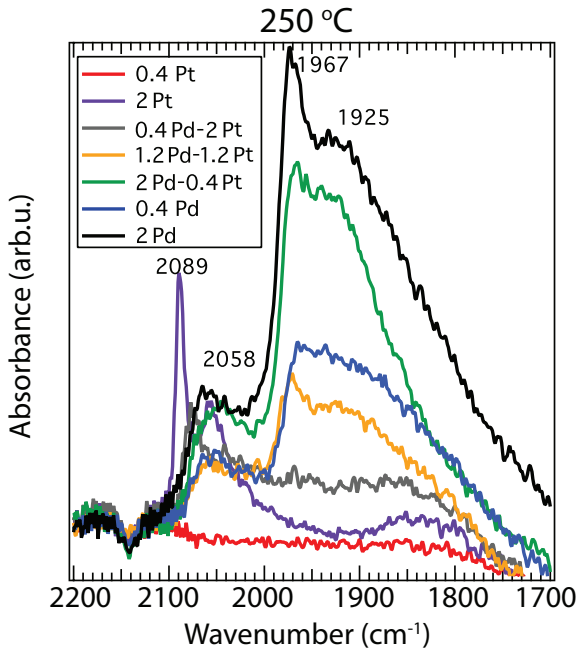

Figure 5: IR absorption spectra in the wavenumber region 1700-2500 cm^{-1} for the Pd, Pt and Pd-Pt catalysts supported on Al_2O_3 and calcined at 800 °C in air and exposed to 1% CO for 5 minutes (reduction phase) at 250 °C.

The CO adsorption measurements on the reduced bimetallic catalysts indicate that CO adsorbs mainly on the Pd sites for the 1.2 Pd-1.2 Pt and 2 Pd-0.4 Pt samples and on the Pt sites for the 0.4 Pd-2 Pt sample, even though some CO adsorption on Pd cannot be excluded for this sample, indicating that Pd segregates to the surface of Pd-Pt particles during reducing conditions. This may indicate a mixed chemical ordering on the Pd-Pt systems with Pd segregation to the surface sites, as previously reported by Bazin et al.[21]

Previous adsorption and reactivity studies of Pd-based catalysts, reported on the CO-induced changes on particles size and shape for the Pd nanoparticles[3] also confirmed by DFT calculations of CO chemisorption on Pd and Pt nanoclusters Pt.[5] Therefore, we cannot exclude that a restructure of particles surface structure may occur in the bimetallic Pd-Pt nanoparticles during CO adsorption. The presented results are supporting our previous findings on the characterisation of the surface structure during reducing conditions of 2 Pd-

0.4 Pt catalyst, which reported that a Pd enriched surface is exposed at the surface of the reduced catalyst.[32] Even more, the results support the alloy formation for the bimetallic Pd-Pt samples calcined at 800 °C as we have previously reported.[9,32] Thus, the method presented in this study can be used to provide information on alloy formation and to characterise the surface of bimetallic catalysts with different surface compositions.

Some previous studies have shown that long CO exposure on Pd/alumina may lead to formation of CO carbide species.[46] Therefore, one could expect a similar situation during the present measurements. Our complementary *in situ* XRD results (not shown) do not show any changes in the unit cell parameters during the same set of experiments, therefore excluding the possibility that such species may form during the low exposure time (5 min).

Conclusions

The surface structure of various bimetallic Pd-Pt catalysts has been characterised using CO as probe molecule by *in situ* FTIR spectroscopy. This spectroscopic study shows that the spectra for bimetallic Pd-Pt catalysts are not superpositions of the corresponding spectra for Pt and Pd, confirming our previous conclusion about PdPt alloy formation for the samples calcined at 800 °C. The results also show that the surface of the alloy particles is enriched with Pd for the reduced catalysts when the Pd:Pt ratio is higher or equal to 2:1 and a Pt enriched surface is exposed when the catalysts contains mainly Pt. The presented method can be used as a starting point to characterise the surface of bimetallic catalysts with different surface compositions.

Acknowledgement

The authors thank MAX IV Laboratory (Lund, Sweden) for providing the beamtime. This work was financially supported by the Swedish Research Council through the Röntgen-Ångström collaborations "Catalysis on the atomic scale" (No. 349-2011-6491) and "Time-

resolved in situ methods for design of catalytic sites within sustainable chemistry" (No. 349-2013-567), the Swedish Foundation for Strategic Research through the project "Novel two-dimensional systems obtained on SiC as a template, for electronics, sensing and catalysis" (RMA15-0024) and the Swedish Energy Agency through the FFI program "Fundamental studies on the influence of water on oxidation catalyst for biogas applications" (No. 40274-1), and partly the Competence Centre for Catalysis, which is financially supported by Chalmers University of Technology, the Swedish Energy Agency and the member companies: AB Volvo, ECAPS AB, Haldor Topsøe A/S, Volvo Car Corporation, Scania CV AB, and Wärtsilä Finland Oy.

Supporting Information Available

Supporting Information containing Figures S1-S4. This material is available free of charge via the Internet at `http://pubs.acs.org/`.

References

(1) Rupprechter, G.; Weilach, C. Spectroscopic Studies of Surface-gas Interactions and Catalyst Restructuring at Ambient Pressure: Mind the Gap! *J. Phys.: Condens. Matter* **2008**, *20*, 184019(17pp).

(2) Yudanov, I.V.; Sahnoun, R.; Neyman, K.; Rösch, N.; Hoffmann, J.; Schauermann, S.; Johanek, V.; Unterhalt, H.; Rupprechter, G.; Libuda, J.; Freund, H.-J. CO Adsorption on Pd Nanoparticles: Density Functional and Vibrational Spectroscopy. *J. Phys. Chem. B* **2003**, *107*, 255-264.

(3) Newton, M.A.; Belver-Coldeira, C.; Martinez-Arias, A.;Fernandez-Garcia, M. Dynamic In situ Observation of Rapid Size and Shape Change of Supported Pd nanoparticles During CO/NO Cycling. *Nature Materials* **2007**, *6*, 528-532.

(4) Fischer-Wolfarth, J.-H.; Farmer, J.A.; Flores-Camacho, J.M.; Genest, A.; Yudanov, I.V.; Rösch, N.; Campbell, C.T.; Schauermann, S.; Freund, H.-J. Particle-size Dependent Heats of Adsorption of CO on Supported Pd Nanoparticles as Mesured with a Single-crystal Microcalorimeter. *Phys. Rev. B* **2010**, *81*, 241416:1-4.

(5) Paz-Borbon, L.O.; Johnston, R.L.; Barcaro, G.; Fortunelli, A. Chemisorption of CO and H on Pd, Pt and Au Nanoclusters: A DFT Aproach. *Eur. Phys. J. D* **2009**, *52*,131-134.

(6) Over, H. Crystallographic Study of Interaction Between Adspecies on Metal Surfaces. *Prog. Surf. Sci.* **1998**, *58*, 249-376.

(7) Sung, S.S.; Hofmann, R. How Carbon Monoxide Bonds to Metal Surfaces. *J. Am. Chem. Soc.* **1985**, *107*, 578-584.

(8) Sheppard, N.; Nguyen, T. T. The Vibrational Spectra of Carbon Monoxide Chemisorbed on the Surface of Metal Catalysts?A Suggested Scheme of Interpretation. In *Advances in Infrared and Raman Spectroscopy*; Clark, R. J. H., Hester, R. E., Eds.; Heyden: London, 1978; Vol. 5; pp. 67-148.

(9) Martin, N.M.; Nilsson, J.; Skoglundh, S.; Adams, E.C.; Wang, X.; Smedler, G.; Raj, A.; Thompsett, D.; Agostini, G., Carlson, S. et al., Study of Methane Oxidation over Alumina Supported Pd-Pt Catalysts Using Operando DRIFTS/ MS and in situ XAS Techniques. *Catalysts, Structure and Reactivity* **2017**, *1-2*, 24-32.

(10) Rousset, J.L.; Stievano, L.; Cadete Santos Aires, F.J.; Geantet, C.; Renouprez, A.j.; Pellarin, M. Hydrogenation of Teralin in the Presence of Sulfur over gamma-Al2O3-Supported Pt, Pd, and Pd-Pt Model Catalysts. *J. Catal.* **2001**, *202*, 163-168.

(11) Narui, K.; Yata, H.; Furuta, K.; Nishida, A.; Kohtoku, Y.; Matsuzaki, T. Effects of Addition of Pt to PdO/Al2O3 Catalyst on Catalytic Activity for Methane Combustion

and TEM Observations of Supported Particles. *Appl. Catal. A: General* **1999**, *179*, 165-173.

(12) Lapisardi, G., Urfels, L., Gelin, P., Primet, M., Kaddouri, A., Garbowski, E., Toppi, S., and Tena, E. Superior Catalytic Behaviour of Pt-doped Pd Catalysts in the Complete Oxidation of Methane at Low Temperature. *Catal. Today*, **2006**, *117*, 564-568.

(13) Ströbel, R.; Grunwaldt, J.-D.; Camenzind, A.; Pratsinis, S. E.; Baiker, A. Flame-made Alumina Supported Pd-Pt Nanoparticles: Structural Properties and Catalytic Behavior in Methane Combustion. *Catal. Lett.* **2005**, *104*, 9-16.

(14) Persson, K.; Eriksson, A.; Jansson, K.; Fierro, J.L.G.; Järås, S. G. Influence of Molar Ratio on Pd-Pt Catalysts for Methane Combustion. *J. Catal.* **2006**, *243*, 14-24.

(15) Chen, M.; Schmidt, L.D. Morphology and Composition of PtPd Alloy Crystallites on SiO2 in Reactive Atmospheres. *J. Catal.* **1979**, *56*, 198-218.

(16) Ozawa, Y.; Tochihara, Y.; Watanabe, A.; Nagai, M.; Omi, S. Deactivation of Pt-PdO/Al2O3 in Catalytic Combustion of Methane. *Applied Catalysis A: General* **2004**, *259(1)*,1-7.

(17) Ishihara T. Effects of Additives on the Activity of Palladium Catalysts for Methane Combustion. *Chem Lett.* **1993**, *22*, 407-410.

(18) Yamamoto, H.; Uchida, H. Oxidation of Methane over Pd and Pt Supported on Alumina in Lean-burn Natural gas Engine Exhaust.*Catal. Today* **1998**, *45*, 147-151.

(19) Niquille-Röthlisberger, A.; Prins, R. Hydrodesulfurization of 4,6-dimethyldibenzothiophene and Dibenzothiophene over Alumina-supported Pt, Pd, and Pt-Pd Catalysts. *J. Catal.* **2006**, *242*, 207-216.

(20) Liu, C.; Shao, Z.; Xiao, Z.; Williams, C.T.; Liang C. Hydrodeoxygenation of Benzofuran

over Silica?Alumina-Supported Pt, Pd, and Pt?Pd Catalysts *Energy Fuels* **2012**, *26*, 4205-4211.

(21) Bazin,D.; Guillaume, D.; Pichon, Ch.; Uzio, D.; Lopez, S. Structure and Size of Bimetallic Palladium-Platinum Clusters in an Hydrotreatment Catalyst. *Oil & Gas Science and Technology-Rev. IFP*, Vol. 60 (2005), No. 5, pp. 801-813.

(22) Paz-Borbon, L.O.; Mortimer-Jones, T.V.; Johnston, R.L.; Posada-Amarillas, A.; Barcaro, G.; Fortunelli, A. Structures and Energetics of 98 Atom Pd-Pt Nanoalloys: Potential Stability of the Leary Tetrahedron for Bimetallic Nnanoparticles. *Phys. Chem. Chem. Phys* **2007**, *9*, 5202?5208.

(23) Massen, C.; Mortimer-Jones, T.V.; Johnston, R.L. Geometries and Segregation Properties of Platinum-Palladium Nanoalloy Clusters. *J. Chem. Soc., Dalton Trans.* **2002**, 4375-4388.

(24) Coq, B.; Figueras, F. Bimetallic Palladium Catalysts: Influence of the Co-metal on the Catalyst Performance. *J. Mol. Catal. A* **2001**, *173*, 117-134.

(25) Johnson, W.C.; Blakely, J.M. Eds. *Interfacial Segregation*; American Society for Metals: Metals Park, OH, 1979.

(26) Chelikowsky, J.R. *Predictions for Surface Segregation in 2.550 Binary Intermetallic Alloys; Research Report;* Exxon Research and Engineering Co.: Linden, NJ.

(27) Du Plessis, J. *Surface Segregation*; Solid State Phenomena; Sci-Tech Publications: Vaduz, Liechtenstein, 1990, Vol. **11**.

(28) Harada, M.; Asakura, K.; Ueki, Y.; Toshima, N. Structure of Polymer-Protected Palladium-Platinum Bimetallic Clusters at the Oxidized State: Extended X-ray Absorption Fine Structure Analysis. *J. Phys. Chem.* **1992**, *96*, 9730-9738.

(29) Hansen, P.L.; Molenbroek, A.M.; Ruban, A.V. Alloy Formation and Surface Segregation in Zeolite-Supported Pd-Pt Bimetallic Catalysts. *J. Phys. Chem. B* **1997**, *101*, 1861-1868.

(30) Van den Oetelaar, L. C. A.; Nooij, O. W.; Oerlemans, S.; Denier van der Gon, A. W.; Brongersma, H.H.; Lefferts, L.; Roosenbrand, A. G.; van Veen, J. A. R. Surface Segregation in Supported Pd-Pt Nanoclusters and Alloys. *J. Phys.. Chem. B* **1998**, *102*, 3445-3455.

(31) Persson, K.; Jansson, K.; Järås, S. Charecterisation and Microstructure of Pd and Bimetallic Pd-Pt Catalysts During Methane Oxidation. *J. Catal.* **2007**, *254*, 401-414.

(32) Martin, N.M.; Nilsson, N.; Skoglundh, M.; Adams, E.C.; Wang, X.; Velin, P.; Smedler, G.; Raj, A.; Thompsett, D.; Brongersma, H.H. *et al.*, Characterization of Surface Structure and Oxidation/Reduction Behavior of Pd-Pt/Al2O3 Model Catalysts. *J. Phys. Chem. C* **2016**, *120*, 28009-28020.

(33) Cerenius, Y. ; Ståhl, K.; Svensson, L.A.; Ursby, T.; Oskarsson, Å.; Albertsson, J.; Liljas, A. The Crystallography Beamline I711 at MAX II. *J. Synchrotron Rad.* **2000**, *7*, 203-208.

(34) Knaapila, M. et al. A New Small-Angle X-ray Scattering Set-up on the Crystallography Beamline I711 at MAX-lab. *J. Synchrotron Rad.* **2009**, *16*, 498-504.

(35) https://icsd.fiz-karlsruhe.de (accessed January 2016)

(36) Radmilovic, V.; Gasteiger, H. A.; Ross Jr, P. N.; Structure and Chemical Composition of a Supported Pt-Ru Electrocatalysis for Methanol Oxidation. *J. Catal.* **1995**, *154*, 98-106.

(37) Schalow, T.; Brandt, B.; Starr, D.E.; Laurin, M.; Shaikhutdinov, S.K.; Schauermann,

S.; Libuda, J.; Freund, H.-J. Size-dependent Oxidation Mechanism of Supported Pd Nanoparticles. *Angew. Chem. Int. Ed.* **2006**, *45*, 3693-3697ă.

(38) Gränzler, A.M.; Casapu, M; Boubnov, A.; Muller, O.; Conrad, S.; Lichtenberg, H.; Frahm, R.; Grunwaldt, J.-D. Operando Spatially and Time-resolved X-ray Absorption Spectroscopy and Infrared Thermography during Oscillatory CO Oxidation. *J. Catal.* **2015**, *328*, 216-224.

(39) Carlsson, P.-A.; Österlund, L.; Thormählen, P.; Palmqvist, A.; Fridell, E.; Jansson, J.; Skoglundh, M. A Transient in situ FTIR and XANES Study of CO Oxidation over Pt/Al2O3 Catalysts. *J. Catal.* **2004**, *226*, 422-434.

(40) Kast, P.; Friedrich, M.; Teschner, D.; Girgsdies, F.; Lunkenbein, T.; Naumann d'Alnoncourt, R.; Behrens, M.; Schlögl, R. CO Oxidation as a Test Reaction for Strong Metal-support Interaction in Nanostructured Pd/FeOx Powder Catalysts. *Appl. Catal. A: General* **2015**, *502*, 8-17.

(41) Rades,T.; Borovkov, V. Yu.; Kazansky, V. B.; Polisset-Thfoin, M.; Fraissard, J. Diffuse Reflectance IR Study of CO Adsorption on a Bimetallic Pt-Pd Catalyst Supported on NaY Zeolite. Evidence of Alloy Formation. *J. Phys. Chem.* **1996**, *100*, 16238-16241.

(42) Rainer, D. R.; Wu, M.-C.; Mahon, D. I.; Goodman, D. W. Adsorption of CO on Pd/Al2O3/Ta(110) Model Catalysts. *J. Vac. Sci. Technol. A* **1996**, *14(3)*, 1184-1188.

(43) Martin, N.M.; van den Bossche, M.; Grönbeck, H.; Hakanoglu, C.; Zhang, F.; Li, T.; Gustafson, J.; Weaver, J.F.; Lundgren, E. CO Adsorption on Clean and Oxidized Pd(111). *J. Phys. Chem. C* **2014**, *118*, 1118-1128.

(44) Becker, E.; Carlsson, P.-A.; Kylhammar, L.; Newton, M. A.; Skoglundh, M. In Situ Spectroscopic Investigation of Low-Temperature Oxidation of Methane over Alumina-Supported Platinum during Periodic Operation. *J. Phys. Chem. C* **2011**, *115*, 944-951.

(45) Primet, M.; de Menorval, L.-C.; Fraissard, J.; Ito, T. Carbon Monoxide Chemisorption on a Pt-NaY Catalyst. Part 2: Influence of Carbon Monoxide Coverage and of Coadsorbed Molecules on the Infrared Spectrum of Adsorbed Carbon Monoxide (Electron Transfer and Dipole-dipole Coupling). *J. Chem. Soc., Faraday Trans. 1* **1985**, *81*, 2867-2874.

(46) Newton, M.A.; Di Michiel, M.; Kubacka, A.; Fernandez-Garcia, M. Combining Time-Resolved Hard X-ray Diffraction and Diffuse Reflectance Infrared Spectroscopy To Illuminate CO Dissociation and Transient Carbon Storage by Supported Pd Nanoparticles during CO/NO Cycling. *J. Am. Chem. Soc.* **2010**, *132*, 4540-4541.

TOC Graphic